Compressed Sensing Based Multi-User Detection with Modified Sphere Detection in Machine-to-Machine Communications

Yalei Ji, Carsten Bockelmann and Armin Dekorsy

Department of Communications Engineering
Otto-Hahn-Alle 1, University of Bremen, 28359 Bremen, Germany
Email: {ji, bockelmann, dekorsy}@ant.uni-bremen.de

Abstract—**Recently, Compressed Sensing has been proposed as a promising physical layer technique for Multi-User Detection in Massive Machine Communication (MMC). MMC is characterized by low data rates, low control signaling overhead and different traffic models compared to human-oriented communication. In this context, Compressed Sensing based Multi-User Detection (CS-MUD) enables efficient direct random access as a potential solution for the massive access problem. Previous work has not considered realistic traffic characteristic. In this work, we consider a typical Poisson traffic model to formulate a MAP detection problem exploiting user sparsity.**

I. INTRODUCTION

Massive Machine Communication (MMC) is expected to grow significantly in coming years [1], posing new requirements for existing communication systems, which are mainly designed for human-oriented communication. One property of MMC is *sporadic transmission*, which means nodes are only occasionally active for data transmission with low data rates. Therefore, it is not well matched to extensive signaling and complex scheduling of current solutions [2]. With a massive number of devices involved, one of the objectives for MMC solutions is to efficiently handle the massive access problem. Due to sporadic transmission, only a few users are occasionally active to transmit data packets with small size, which makes high control signaling inefficient. Previous literature shows that MUD in MMC can be formulated as a sparse detection problem with modeling user inactivity [3]. Thus, Compressed Sensing based Multi-User Detection (CS-MUD) can be applied to jointly detect activity and data at the receiver, which reduces control signaling since the activity of all users does not need to be signaled to the receiver anymore.

Previously, a very simplified model has been used to describe the user activity. In [3] a simple Bernoulli model is considered. Each user is independently active with the same low probability p_a, which is not accurate enough to model the traffic pattern in MMC systems. In this paper, we exploit the probability mass function of the sparse multi-user signal through a more realistic traffic model. For the purpose of more realistic traffic modeling, a Poisson model will be considered here. Therefore, a new MAP detection problem is formulated and in order to solve this MAP problem, a modified sphere detector will be proposed. Finally, a sorting approach for complexity reduction is discussed.

The reminder of this paper is organized as follows: Section II presents the general system description in the context of multi-user uplink transmission as the basis of the investigation. Section III formulates the MAP detection problem w.r.t. different traffic models. The analysis of our algorithms is given in Section IV. In Section V, we investigate an over-determined CDMA system as an example to verify the analysis in Section IV. Finally, the paper is concluded in Section VI.

II. SYSTEM DESCRIPTION

In this paper, an uplink scenario is considered with K nodes transmitting data to a central Base Station (BS), as shown in Fig. 1. The BS is capable of advanced signal processing, such as detecting signals and aggregating messages for further application while the node devices are low complexity. We assume that nodes are only occasionally active, e.g., packets might be transmitted to the BS event driven. During the active time, each node will transmit data packets of small size. Meanwhile, the BS is active all the time in order to listen to the information coming from all active nodes.
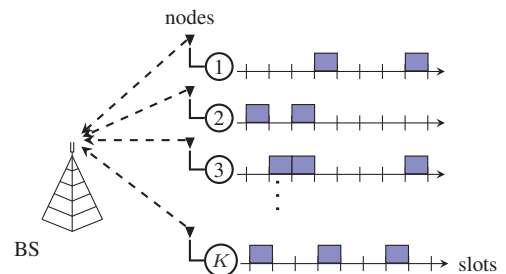

Figure 1: Sporadic uplink transmission of multiple devices communicating with a BS. Each time slot corresponds to one data frame and the system is assumed to be synchronous.

Herein, we assume all users are synchronized on a slot basis, which means users switch activity on the same symbol time basis. Accordingly, active users transmit a frame of symbols per slot but we focus on the detection of one single symbol per user. The uplink transmission model can be described by the linear input-output relation at the symbol clock as

$$\mathbf{y} = \mathbf{T}\mathbf{x} + \mathbf{n}, \tag{1}$$

where the stacked vector $\mathbf{x}$ contains all the symbols from all K nodes in one same slot. To incorporate node inactivity, we

model an inactive node as "transmitting" a zero and active nodes select data symbol from a modulation alphabet $\mathcal{A}$, where $\mathcal{A}$ represents a discrete modulation alphabet, e.g., Binary Phase Shift Keying (BPSK). Consequently, the elements of vector $\mathbf{x}$ belong to the so called augmented symbol alphabet $\mathcal{A}_0 = \mathcal{A} \bigcup \{0\}$. Matrix $\mathbf{T}$ summarizes the influences of channel and medium access between the nodes and BS. For example, it represents both the spreading and channel convolution in CDMA systems. Here, we assume that we have a fully loaded or over-determined system, which means that the number of rows of $\mathbf{T}$ is equal or larger than the number of columns in it. Finally, $\mathbf{n}$ denotes additive white Gaussian noise with zero mean and variance σ_{n}^2 and the vector $\mathbf{y}$ represents the measurements of signal $\mathbf{x}$ at the receiver.

In *sporadic communication*, the basic assumption is intermittent (sporadic) user activity, which usually leads to a small number of active users compared to the total number of users. Consequently, there will be only a few number of non-zero entries in vector $\mathbf{x}$, which enables the ideas from sparse signal processing and CS. In the following, we will consider the sparsity exploiting sphere detector to solve the MAP detection problem for (1) under the assumption of two well-known different traffic models, which determine the statistical properties of $\mathbf{x}$.

A. Bernoulli Model

From the user perspective, all nodes are independent and each of them can be assigned a certain activity probability. If we assume all user have the same activity probability p_{a}, the active users will transmit data with $\Pr(x_k \in \mathcal{A}) = p_{\mathrm{a}}$, while inactive nodes are modeled with $\Pr(x_k = 0) = 1 - p_{\mathrm{a}}$. Consequently, for synchronous transmission, the joint probability distribution for vector $\mathbf{x}$ can be formulated as

$$\Pr\{\mathbf{x}\} = (1 - p_{\mathrm{a}})^{K - \|\mathbf{x}\|_0} \left(\frac{p_{\mathrm{a}}}{|\mathcal{A}|} \right)^{\|\mathbf{x}\|_0}, \qquad (2)$$

where $\|\mathbf{x}\|_0$ denotes the zero-"norm" counting the number of non-zero entries in $\mathbf{x}$ and $|\mathcal{A}|$ is the cardinality of the modulation alphabet used for data transmission. This model has been already well exploited in former works in [3], [4] and here is used for performance comparison.

B. Poisson Model

The Bernoulli model is very simple but not realistic and accurate enough for the traffic modeling. It has been shown that traffic of MMC communications can be modeled via Poisson models [5], whose joint probability distribution can be described as

$$\Pr\{\mathbf{x}\} = \frac{\lambda^{\|\mathbf{x}\|_0} e^{-\lambda}}{\|\mathbf{x}\|_0! \binom{K}{\|\mathbf{x}\|_0}}, \qquad (3)$$

where λ is the rate parameter, denoting the mean number of active nodes. The solution of the MAP detection problem with (3) as a priori information is one of our goals in this work.

III. Problem Formulation

Given the input-output relation in (1), a MAP detector can be formulated to estimate signal $\mathbf{x}$. In general, the system matrix $\mathbf{T}$ has to be estimated at the receiver, e.g., via training

sequences [6]. Here we assume the perfect knowledge of matrix $\mathbf{T}$ at the receiver. In [3], a general form of MAP detection, which is regularized by a priori information is given as

$$\hat{\mathbf{x}}_{\mathrm{opt}} = \arg \min_{\mathbf{x} \in \mathcal{A}_0} \|\mathbf{y} - \mathbf{T}\mathbf{x}\|_2^2 - \sigma_{\mathrm{n}}^2 \log \Pr\{\mathbf{x}\}, \qquad (4)$$

where the penalty term is scaled by the noise variance σ_{n}^2.

Usually, if the term, $-\sigma_{\mathrm{n}}^2 \log \Pr\{\mathbf{x}\}$, is monotonically increasing, the problem in (4) can be efficiently solved by a Sparsity Aware Sphere Detector (SA-SD) [3]. In case of different traffic models, (4) can be reformulated w.r.t (2) and (3). For simplicity, a BPSK modulated alphabet is applied here with the augmented alphabet $\mathcal{A}_0 = \{\pm 1\} \cup \{0\}$ and therefore, we have $|\mathcal{A}| = 2$. The sparsity aware MAP detection problem w.r.t. (2) is given as

$$\hat{\mathbf{x}}_{\mathrm{opt}} = \arg \min_{\mathbf{x} \in \mathcal{A}_0} \|\mathbf{y} - \mathbf{T}\mathbf{x}\|_2^2 + \sigma_{\mathrm{n}}^2 \|\mathbf{x}\|_0 \log \left(\frac{1 - p_{\mathrm{a}}}{p_{\mathrm{a}}/2} \right), \qquad (5)$$

which has already been well exploited and the validity of SA-SD for solving (5) has been proved and can be found in [3], [7].

Similar to Bernoulli model, if we reformulate the MAP problem in (4) using (3), naturally a different cost function results

$$\hat{\mathbf{x}}_{\mathrm{opt}} = \arg \min_{\mathbf{x} \in \mathcal{A}_0} \|\mathbf{y} - \mathbf{T}\mathbf{x}\|_2^2 + \sigma_{\mathrm{n}}^2 \log \left\{ \frac{K! e^{\lambda}}{\lambda^{\|\mathbf{x}\|_0} (K - \|\mathbf{x}\|_0)!} \right\}. \qquad (6)$$

As mentioned earlier, the cost function (6) has to be monotonically increasing to allow for a sphere detector implementation. In the next section, the analysis for the application of sphere detector w.r.t. Poisson model will be presented.

IV. Analysis

In this section, a new sphere detector exploiting signal sparsity for solving the MAP problem given as (6), named Poisson based SA-SD (P-SA-SD), will be analyzed. For the purpose of better comparison, we name the SA-SD for (5) as Bernoulli SA-SD (B-SA-SD) in this work.

In order to simplify the complex mathematical expression in the analysis, we use the following shorthand to represent the a priori part in (6).

$$\mathcal{P}\{\|\mathbf{x}\|_0, \lambda, K\} = \log \left\{ \frac{K! e^{\lambda}}{\lambda^{\|\mathbf{x}\|_0} (K - \|\mathbf{x}\|_0)!} \right\} \qquad (7)$$

A. Poisson based SA-SD

Assuming $\mathbf{T}$ with full rank in an over-determined or fully loaded system, QR decomposition can be used to reformulate the MAP problem (6). Using $\mathbf{T} = \mathbf{Q}\mathbf{R}$ where $\mathbf{R}$ is a upper triangular matrix and $\mathbf{Q}$ is an unitary matrix, we get

$$\hat{\mathbf{x}}_{\mathrm{opt}} = \arg \min_{\mathbf{x} \in \mathcal{A}_0} \|\mathbf{Q}^H \mathbf{y} - \mathbf{Q}^H \mathbf{Q}\mathbf{R}\mathbf{x}\|_2^2 + \sigma_{\mathrm{n}}^2 \mathcal{P}\{\|\mathbf{x}\|_0, \lambda, K\} \qquad (8)$$

$$= \arg \min_{\mathbf{x} \in \mathcal{A}_0} \|\mathbf{y}' - \mathbf{R}\mathbf{x}\|_2^2 + \sigma_{\mathrm{n}}^2 \mathcal{P}\{\|\mathbf{x}\|_0, \lambda, K\}. \qquad (9)$$

Here, $\mathbf{y}'$ represents the filtered received signal by matrix $\mathbf{Q}^H$ not changing the estimation problem. testing all the

possible hypotheses for each symbol in $\mathbf{x}$. of (9), will be our final optimal solution $\hat{\mathbf{x}}_{\text{opt}}$. As we mentioned above, for the purpose of applying sphere detection, we need to prove the a priori part together with the maximum-likelihood term to be monotonically increasing. For this purpose, we reform the cost function as

$$\hat{\mathbf{x}}_{\text{opt}} = \arg\min_{\mathbf{x} \in \mathcal{A}_0} \sum_{k=1}^{K} \left\{ (y'_k - \sum_{l=k}^{K} R_{lk} x_l)^2 + \sigma_{\text{n}}^2 \mathcal{P}\{|x_k|_0, \lambda, K\} \right\}. \tag{10}$$

Apparently, the cost of the maximum-likelihood term for the jth layer is given by

$$\zeta^j = |y'_j - \sum_{i=j}^{K} \mathbf{R}_{ji} x_i|_2 \tag{11}$$

The second step is to calculate the a priori cost for the jth layer. Firstly, we rewrite the a priori term as

$$\mathcal{P}\{\|\mathbf{x}\|_0, \lambda, K\} = \log \left\{ \frac{\overbrace{K! e^{\lambda}}^{\text{constant}}}{\underbrace{\lambda^{\|\mathbf{x}\|_0} (K - \|\mathbf{x}\|_0)!}_{\text{variable}}} \right\}, \tag{12}$$

where the nominator can be ignored in the analysis as it is constant. Thus, only the denominator remains to be considered. The variable part can be rewritten further as

$$\mathcal{P}\{\|\mathbf{x}\|_0, \lambda, K\} = C - \underbrace{\|\mathbf{x}\|_0 \log \lambda}_{d_1} - \underbrace{\log\{(K - \|\mathbf{x}\|_0)!\}}_{d_2}. \tag{13}$$

We define $\tilde{\mathcal{P}}\{\|\mathbf{x}\|_0, \lambda, K\} = \mathcal{P}\{\|\mathbf{x}\|_0, \lambda, K\} - C$ as the remaining cost term, given as

$$\tilde{\mathcal{P}}\{\|\mathbf{x}\|_0, \lambda, K\} = -\underbrace{\|\mathbf{x}\|_0 \log \lambda}_{d_1} - \underbrace{\log\{(K - \|\mathbf{x}\|_0)!\}}_{d_2}. \tag{14}$$

The sphere detector calculates the cost of (13) layer by layer. Therefore, considering the jth layer in the detector with $1 \leq j \leq K$, we have to differentiate two cases. In the first case, the SD calculates the cost of jth layer for hypothesis $x_j = 0$. Then the zero-"norm" $\|\mathbf{x}\|_0^{j-1}$ stays constant, i.e., $\|\mathbf{x}\|_0^{j-1} = \|\mathbf{x}\|_0^j$. Consequently, the overall a priori cost up to the jth layer is given as

$$d_1^j|_{x_j=0} = (\|\mathbf{x}\|_0^{j-1} + 0) \log \lambda = \|\mathbf{x}\|_0^{j-1} \log \lambda, \tag{15}$$
$$d_2^j|_{x_j=0} = \log\{(K - (\|\mathbf{x}\|_0^{j-1} + 0))!\} = \log\{(K - \|\mathbf{x}\|_0^{j-1})!\}, \tag{16}$$

with no change of cost from the $(j-1)^{\text{th}}$ to j^{th} layer. In the other case, if we assume $x_j = \pm 1$, we have $\|\mathbf{x}\|_0^j = \|\mathbf{x}\|_0^{j-1} + 1$. Thus, the two cost terms are given as

$$d_1^j = (\|\mathbf{x}\|_0^{j-1} + 1) \log \lambda = d_1^{j-1} + \log \lambda, \tag{17}$$
$$d_2^j = \log\{(K - (\|\mathbf{x}\|_0^{j-1} + 1))!\} = d_2^{j-1} - \log(K - \|\mathbf{x}\|_0^{j-1}). \tag{18}$$

Here, (18) is from the properties of factorial and logarithm. Finally, recalling the minus sign in (13), the increment of a priori cost from $(j-1)^{\text{th}}$ layer to j^{th} layer is

$$\triangle d_{\text{a}}|_{j-1}^j = \begin{cases} 0, & x_j = 0 \\ \log(\frac{K - \|\mathbf{x}\|_0^{j-1}}{\lambda}), & x_j = \pm 1 \end{cases}$$

Therefore, considering the maximum-likelihood cost, the overall cost in j^{th} layer can be given as

$$\triangle d|_{j-1}^j = \zeta^j + \triangle d_{\text{a}}|_{j-1}^j. \tag{19}$$

Accordingly, to prove monotonicity the following inequality should hold.

$$\triangle d|_{j-1}^j \geq 0 \tag{20}$$

Given the analysis above, we get

$$\sigma_{\text{n}}^2 \log(\frac{K - \|\mathbf{x}\|_0^{j-1}}{\lambda}) + \zeta^j \geq 0, \tag{21}$$

considering a specific signal-to-noise ratio (SNR). Furthermore, it can be reformed to

$$\|\mathbf{x}\|_0^{j-1} \leq K - \lambda \cdot e^{(-\frac{1}{\sigma_{\text{n}}^2} \zeta^j)}. \tag{22}$$

Considering the constraint given in (22), the zero-"norm" $\|\mathbf{x}\|_0^{j-1}$ for the $(j-1)^{\text{th}}$ layer should fulfill the inequality to ensure a monotonic increase of the cost at the jth layer. Eq. (22) has to be fulfilled for every step of the tree search facilitated by sphere detection to achieve a MAP estimate. Unfortunately, it cannot be guaranteed that the sphere detector does not visit branches that violate (22). However, it is well known from literature that even in low SNR cases the worst case behavior of the sphere detector will still be better than exhaustive search. Thus, for very low λ it is reasonable to assume that sparse solutions will still be preferred. To this end, the SNR in the inequality needs also to be considered. If we consider a general constraint covering all elements in $\mathbf{x}$ up to layer $K - 1$, it can be given as

$$\|\mathbf{x}\|_0^{K-1} \leq K - \lambda \cdot e^{(-\frac{1}{\sigma_{\text{n}}^2} \zeta^K)}. \tag{23}$$

Clearly, this constraint highly depends on the current SNR, i.e., $1/\sigma_{\text{n}}^2$. Specifically, if we have a extremely high SNR with $\sigma_{\text{n}}^2 \to 0$, there will be no effect from the a priori part. We will simply have a maximum likelihood detection problem with condition

$$\|\mathbf{x}\|_0^{K-1} \leq K, \tag{24}$$

which will always be fulfilled. However, on the other hand, if we are facing a quite low SNR with $\sigma_{\text{n}}^2 \to \infty$, the constraint will turn out to be

$$\|\mathbf{x}\|_0^{K-1} \leq K - \lambda. \tag{25}$$

This is clearly the worst condition that can be used to check for an optimal solution. Even though the condition cannot be guaranteed, the sphere detector can still be modified to solve the MAP problem for the Poisson model. In following part, we have some numerical results showing how the a priori cost behaves given different K and λ.

Fig. 3a and Fig 3b show the results of different λ given $K = 10, 100$. As we can see, with low λ, the a priori cost can be ensured to be monotonically increasing. For example, when $K = 10$ and $\lambda = 1$, there will be no decrease for $\mathcal{P}\{\|\mathbf{x}\|_0, \lambda = 1, K = 10\}$ even if the sphere detector runs through all the hypotheses. However, in the case of $\lambda = 2$, there is small region where $\mathcal{P}\{\|\mathbf{x}\|_0, \lambda = 1, K = 10\}$ decreases. Specifically, as shown in Fig. 2, the sphere detector will run all the hypotheses $\{\pm 1, 0\}$ for each layer. Here, the value in each branch represents one hypothesis for each symbol

in $\mathbf{x}$. Considering the estimate for K layers, $\mathbf{x}^K$ might reach the case of all elements choosing candidates from $\{\pm 1\}$. As a consequence, the cost will decrease. However this case will hopefully only happen with low probability and will not occur if the sphere detector converges to the sparse solution. To decrease the probability even further we will propose a sorting strategy, which will be introduced in the next section. Similar observations can be drawn for $K = 100$. Thus, Fig. 3 can be used as an indication showing which λ will be acceptable.
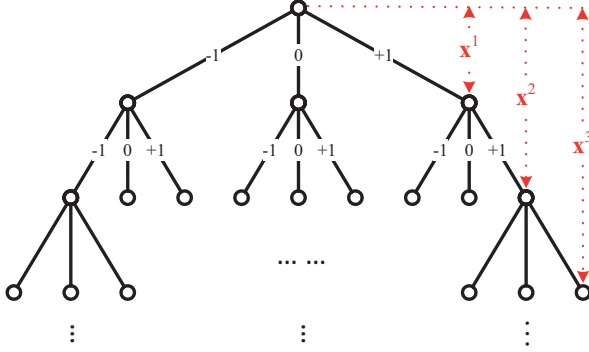

Figure 2: Search tree for sphere detection with $\mathbf{x}^j$ indicating the current estimate with all hypotheses up to the jth layer.

(a) $K = 10$, cost

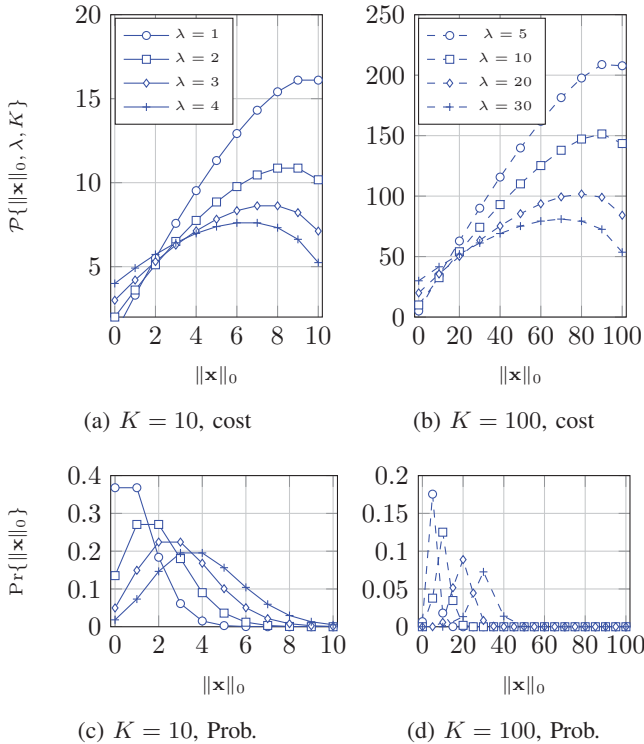(b) $K = 100$, cost

(c) $K = 10$, Prob.

(d) $K = 100$, Prob.

Figure 3: Examples for the evaluation of penalty term $\mathcal{P}\{\|\mathbf{x}\|_0, \lambda, K\}$ with different rate parameters λ and K; Correspondingly, the probability mass function for different λ is given in the lower part.

B. Correlation Sorted Sphere Detector

As an optimum method to solve (4), sphere detection is still of high complexity even in low system dimension. As shown in [8], sorting can be used to efficiently reduce the complexity of sphere detection. Additionally, the a priori cost given by (7) will probably not reach the decreasing region if the sphere detector can find the active users in the first layers with high probability leading to zeros in the lower layers. Therefore, we propose a sorted sphere detector to reduce the complexity and also make sure the solution of (6) converges quickly to the solution.

In [9], Orthogonal Matching Pursuit (OMP) has been presented as a popular algorithm with low complexity in CS-MUD. OMP is a greedy CS algorithm, which exploits the correlation between the received signal $\mathbf{y}$ and the system matrix $\mathbf{T}$. The correlation between $\mathbf{y}$ and $\mathbf{T}$ is given by

$$\mathbf{c}_\mathrm{n} = |\mathbf{T}_\mathrm{n}^H \mathbf{y}|, \qquad (26)$$

where $\mathbf{T}_\mathrm{n}$ represents the system matrix, whose columns are normalized to unit vectors [10]. The columns in $\mathbf{T}_\mathrm{n}$, whose correlations with $\mathbf{y}$ are higher, are considered having higher probability to be active. From the perspective of sphere detection, the detector starts from the root to check the augmented alphabet $\mathcal{A}_0$, which is also the Kth element in $\mathbf{x}$. Thus, our idea is to enforce the detector to start from the layer with highest correlation and follow in descending correlation order, which potentially saves effort in searching the nodes with minimum cost. Therefore, we use the correlation as defined in (26) to sort the system matrix $\mathbf{T}$.

The specifics of the sorted P-SA-SD are given by Alg. 1. Due to the sorting, active users are detected in the first layers of the search tree with high probability, as shown in Fig. 2. Therefore, condition (23) is less likely violated as the remaining layers are zeros with high probability.

Algorithm 1 Correlation sorted P-SA-SD

Require: $\mathbf{y}$, $\mathbf{T}_\mathrm{n}$, σ_n^2, λ, K
  $\mathbf{c}_\mathrm{n} \leftarrow |\mathbf{T}_\mathrm{n}^H \mathbf{y}|$
  Index $\leftarrow$ sort($\mathbf{c}_\mathrm{n}$, 'ascend');
  $\tilde{\mathbf{T}} \leftarrow \mathbf{T}(\mathrm{Index})$;
  $\tilde{\mathbf{Q}}, \tilde{\mathbf{R}} \leftarrow$ qr($\tilde{\mathbf{T}}$);
  $\tilde{\mathbf{y}} \leftarrow \tilde{\mathbf{Q}}^H \mathbf{y}$;
  for $k = K, \cdots, 1$ **do**
    for all $x_k \in \mathcal{A}_0$ **do**
      $\zeta^k \leftarrow \sum_{k=1}^K \left(\tilde{y}_k - \sum_{l=k}^K r_{kl} x_l \right)^2$;
      $d_\mathrm{a}^k \leftarrow \sigma_\mathrm{n}^2 \left(\mathcal{P}\{\|\hat{\mathbf{x}}\|_0^k | \lambda, K\} \leftarrow \|\hat{\mathbf{x}}\|_0^k \right)$;
      $d_x \leftarrow \zeta^k + d_\mathrm{a}^k - d_\mathrm{a}^{k-1}$;
    end for
    $\hat{x}_k \leftarrow \arg\min_{\forall x_k \in \mathcal{A}_0} d_x$
  end for
  $\hat{\mathbf{x}}_{\mathrm{opt}}(\mathrm{Index}) \leftarrow \hat{\mathbf{x}}_{\mathrm{opt}}$;
  return $\hat{\mathbf{x}}$

V. PERFORMANCE EVALUATION

A. Setup

In order to verify the analysis in Section IV, an overdetermined system with $K = 10$ user nodes with CDMA [11]

as the medium access scheme and spreading sequence length of $N_\text{s} = 16$ is considered in this section. The case of under-determined CDMA systems is beyond the scope of discussion in this paper while the extension is also possible [7]. Furthermore, each active node is assumed to transmit a BPSK modulated symbols every time. Specifically, the symbols of active nodes are spread to chips by a node-wise spreading code and transmitted over a frequency selective Rayleigh fading channel modeled as $L_\text{h} = 6$ independent and identically Rayleigh distributed taps with exponential decaying power delay profile. For simplicity, we assume the nodes to transmit synchronously in time and the convolution of user-specific spreading and the channel effects is summarized by matrix $\mathbf{A} \in \mathbb{C}^{(N_\text{s}+L_\text{h}-1)\times K}$. A matched filter is applied at the BS to go from chip rate back to symbol rate. In this setup, perfect channel state information is assumed at the receiver, which can be obtained by periodic training phases. Meanwhile, a pre-whitening filter $\mathbf{P} \in \mathbb{C}^{K \times K}$ is deployed to ensure uncorrelated white Gaussian noise and capture the symbol-rate input-output relation as follows.

$$\begin{aligned} \mathbf{y} &= \mathbf{P}\mathbf{A}^H\mathbf{A}\mathbf{x} + \mathbf{P}\mathbf{A}^H\mathbf{n} \\ &= \mathbf{T}\mathbf{x} + \tilde{\mathbf{n}}. \end{aligned} \tag{27}$$

The details of applying the matched filtering and pre-whitening filter can be found in [12]. We have vector $\mathbf{y} \in \mathbb{C}^K$ and matrix $\mathbf{T} \in \mathbb{C}^{K \times K}$ effectively summarizing the influences from spreading, channel and filtering at the receiver. The setup for the simulation in this paper is given as follows.

Simulation Parameters	
# of Nodes	$K = 10$
Spreading Gain	$N_\text{s} = 16$
Channel Impulse Resp.	$L_\text{h} = 6$ taps
Channel Type	complex-value Rayleigh fading
Modulation Type	BPSK
Channel State Information	Perfect
Activity Model	Bernoulli($p_\text{a} = 0.2$) Poisson($\lambda = 2$)

B. Activity and Data Detection

In this work, we use an augmented alphabet $\mathcal{A}_0 = \{\pm 1, 0\}$ for data modulation and it indicates both the user activity and data. The performance evaluation is based on $\mathcal{A}_0 = \{\pm 1, 0\}$ and we take the Symbol Error Rate (SER), which includes both activity and data detection errors, as performance indicator. In this part, the oracle SER shows the case of perfect user activity knowledge known at the receiver for comparison.

Fig. 4 shows the results of the P-SA-SD, which was introduced in Section IV. In order to clearly see the validity of the P-SA-SD, we also apply the B-SA-SD for the Poisson traffic model, which originally has been developed for the Bernoulli model. Due to the model mismatch of B-SA-SD, we have a slight performance gain compared to the P-SA-SD shown by the blue curve with squares. Here, the oracle case is plotted for baseline comparison with perfect knowledge of user activity at the BS demonstrating the loss by sphere detection.
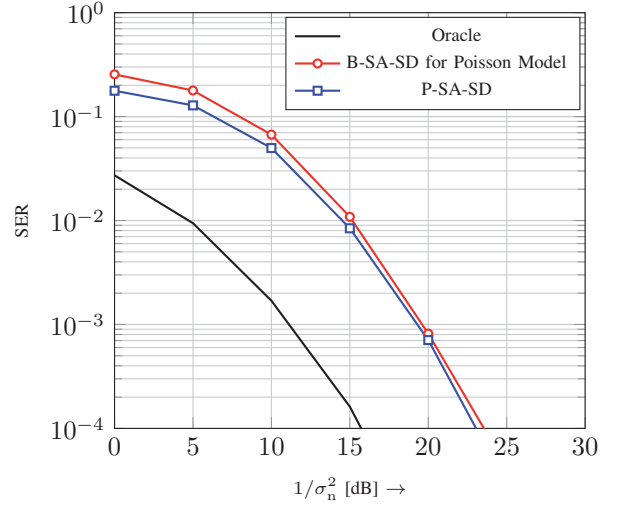

Figure 4: SER results for MAP detection given in (6) with P-SA-SD and the B-SA-SD applied for the Poisson model here for comparison.

Fig. 5 presents the results of Sphere Detector with sorting, which will be named as sorted SA-SD, for both Bernoulli and Poisson models. In general, the Bernoulli and Poisson models have almost the same SER results because the activity probability of Bernoulli model is set to be $p_\text{a} = 0.2$, which is the same as the rate parameter $\lambda = 2$ in Poisson model, given $K = 10$ nodes. Apparently, the sorted SA-SD achieves the same performance as the unsorted SA-SD in Bernoulli model and the same is true for the Poisson model. However, there is still a large gap to the oracle case, which is mainly determined by the activity detection errors. While the sorting results in the same SER performance it will decrease the complexity as shown in the following.
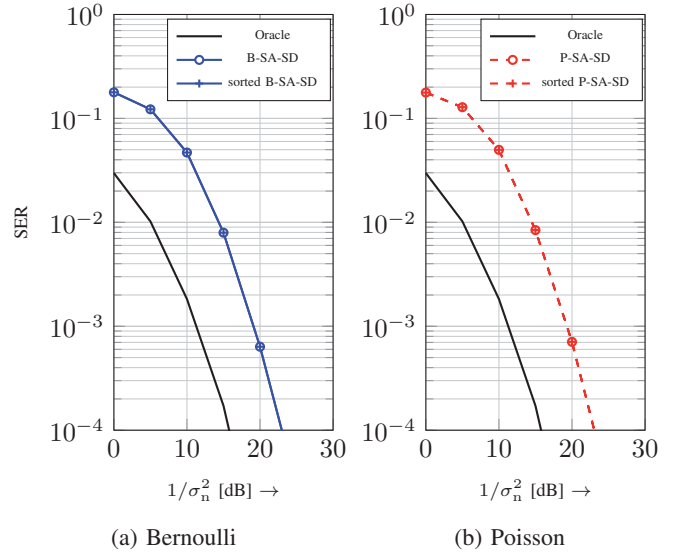

(a) Bernoulli

(b) Poisson

Figure 5: a), SER results for B-SA-SD with or without sorting; b) SER results for P-SA-SD with or without sorting.

C. Complexity Comparison

Fig. 6 plots the complexity of B-SA-SD and P-SA-SD as the number of visited nodes respectively. Specifically, the number of nodes in each layer of sphere detection is determined by the augmented alphabet $\mathcal{A}_0$. Each checked hypothesis means one more visited node in the complexity results. As shown in Fig. 6, the correlation sorting highly reduces the complexity in the range of low SNR but in the high SNR range all the curves converge. Therefore, the sorting gives us the same SER performance as introduced in last section as well as significantly reduces the complexity of sphere detector.
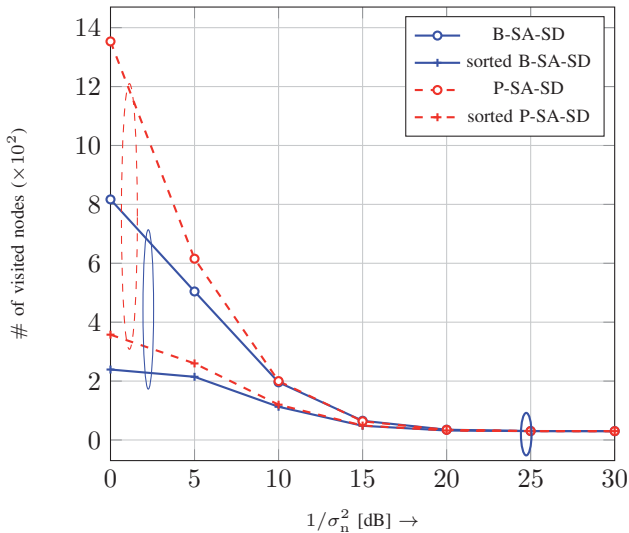

Figure 6: Complexity comparison for P-SA-SD and B-SA-SD with or without sorting in terms of the number of visited nodes.

VI. CONCLUSION

In this paper, a study of modified sphere detection methods is presented w.r.t. different traffic models in MMC communication systems on the basis of Compressed Sensing based Multi-User Detection. The Poisson based Sparsity-Aware Sphere Detection (P-SA-SD) optimally solves the maximum a posteriori detection problem for the Poisson model with higher probability. Furthermore, we introduced a correlation based sorting for the proposed P-SA-SD that leads to a significant decrease of complexity.

ACKNOWLEDGEMENT

REFERENCES

[1] A. Bartoli, M. Dohler, J. Hernández-Serrano, A. Kountouris, and D. Barthel, "Low-power low-rate goes long-range: The case for secure and cooperative machine-to-machine communications," in *Proceedings of the IFIP TC 6th International Conference on Networking*, ser. NETWORKING'11, 2011.

[2] P. Jain, P. Hedman, and H. Zisimopoulos, "Machine Type Communications in 3gpp Systems," *Communications Magazine, IEEE*, vol. 50, no. 11, pp. 28–35, November 2012.

[3] H. Zhu and G. B. Giannakis, "Exploiting Sparse User Activity in Multiuser Detection," *IEEE Trans. Commun.*, vol. 59, no. 2, pp. 454–465, February 2011.

[4] C. Bockelmann, H. Schepker, and A. Dekorsy, "Compressive Sensing based Multi-User Detection for Machine-to-Machine Communication," *Transactions on Emerging Telecommunications Technologies*, vol. 24, no. 4, pp. 389–400, Jun 2013.

[5] 3GPP, "Service Requirements for Machine-Type Communications," Technical report TR 22.368, 2012.

[6] H. Schepker, C. Bockelmann, and A. Dekorsy, "Exploiting Sparsity in Channel and Data Estimation for Sporadic Multi-User Communication," in *10th International Symposium on Wireless Communication Systems (ISWCS 13)*, Ilmenau, Germany, Aug 2013.

[7] F. Monsees, C. Bockelmann, D. Wübben, and A. Dekorsy, "Compressed Sensing Bayes Risk Minimization for Under-determined Systems via Sphere Detection," in *2013 IEEE 77th Vehicular Technology Conference (VTC2013-Spring)*, Dresden, Germany, Jun 2013.

[8] B. Knoop, F. Monsees, C. Bockelmann, D. Wübben, S. Paul, and A. Dekorsy, "Sparsity-Aware Successive Interference Cancellation with Practical Constraints," in *17th International ITG Workshop on Smart Antennas (WSA 2013)*, Stuttgart, Germany, Mar 2013.

[9] Y. Pati, R. Rezaiifar, and P. Krishnaprasad, "Orthogonal Matching Pursuit: Recursive Function Approximation with Applications to Wavelet Decomposition," *Signals, Systems and Computers*, vol. 1, pp. 40–44, November 1993.

[10] T. Hastie, R. Tibshirani, and J. Friedman, *The Elements of Statistical Learning*, ser. Springer Series in Statistics. Springer New York Inc., 2001.

[11] S. Verdú, *Multiuser Detection*. Cambridge, U.K.: Cambridge Univ. Press, November 1998.

[12] F. Monsees, C. Bockelmann, D. Wübben, and A. Dekorsy, "Sparsity Aware Multiuser Detection for Machine to Machine Communication," in *Second International Workshop on Machine-to-Machine Communication at IEEE Globecom 2012*, Anaheim, USA, Dec 2012.